CORROSION SCIENCE AND TECHNOLOGY, Vol.16, No.1(2017), pp.8~14
[Research Paper]
pISSN: 1598-6462 / eISSN: 2288-6524
DOI: https://doi.org/10.14773/cst.2017.16.1.8

Corrosion Behavior and Oxide Film Formation of T91 Steel under Different Water Chemistry Operation Conditions

D. Q. Zhang[1,†], C. Shi[1], J. Li[1], L. X. Gao[1], and K. Y. Lee[2]

[1]*Department of Environmental Engineering, Shanghai University of Electric Power, Shanghai 200090, PR China*
[2]*State Key Laboratory of Structural Analysis for Industrial Equipment, Department of Engineering Mechanics, Dalian University of Technology, Dalian 116024, P R China*

(Received June 07, 2016; Revised January 18, 2017; Accepted January 20, 2017)

The corrosion behavior of a ferritic/martensitic steel T91 exposed to an aqueous solution containing chloride and sulfate ions is investigated depending on the stimulated all-volatile treatment (AVT) and under oxygenated treatment (OT) conditions. The corrosion of T91 steel under OT condition is severe, while the corrosion under AVT condition is not. The co-existence of chloride and sulfate ions has antagonistic effect on the corrosion of T91 steel in both AVT and OT conditions. Unlike to corrosion resistance in the aqueous solution, OT pretreatment provides T91 steel lower oxidation-resistance than VAT pretreatment. From scanning electron microscopy/energy dispersive X-ray spectroscopy (SEM/EDS) and X-ray diffraction (XRD) analysis, the lower corrosion resistance in the aqueous solution by VAT conditions possibly is due to the formation of pits. In addition, the lower oxidation resistance of T91 steel pretreated by OT conditions is explained as follows: the cracks formed during the immersion under OT conditions accelerated peeling-off rate of the oxide film.

Keywords: *T91 steel, oxidation, corrosion, electric power plant*

1. Introduction

T91 alloy, 9Cr–1Mo ferritic/martensitic steel has been widely used as tube material for heater or super-heater in the thermal power equipment due to its excellent creep resistance and low thermal expansion coefficients[1]. Boiler tube failure is one of the major damage factors affecting the structure integrity of equipment. T91 steel can undergo pitting corrosion caused by aggressive ions, such as sulfate ions (SO_4^{2-}) and chloride ions (Cl^-). The SO_4^{2-} and Cl^- concentrations can increase in power plants as a result of condenser leakage into feedwater system, the dissolution of ion exchange resins, and the decomposition of organics. On the other hand, T91 steel has been exposed to the overheated steam, which caused oxidation problems. Corrosion and oxide scale formation on tube surfaces significantly influence operational reliability of thermal power plant boilers, which can lead to heat transfer decreasing, overheating and tube failures, loss of turbines efficiency, and diverse damages in other segments of power units.

Water chemistry has an important influence on the corrosion of the thermal equipment[2]. Water chemistry control is beneficial to prevent and/or reduce corrosion in boiler system and to minimize the transport of corrosion products and corrosive contaminants to the boiler. The current chemistry control strategy involves all volatile treatment (AVT) and oxygenated water treatment (OT). The AVT relies on complete removal of oxygen (< 5 ppb) using hydrazine as an oxygen scavenger with the $pH_{25\,℃}$ adjusted to about 9 using ammonia. In OT operation, oxygen is added to the demineralized (< 0.2 μ Scm^{-1}) alkaline ($pH_{25\,℃}$ = 8.0 ~ 8.5 (ammonia)) feed water to keep the oxygen level between 30 ~ 50 ppb < 0.2. The OT promotes the formation of the stable protective magnetite (Fe_3O_4) layer, which reduces water-steam-side corrosion behavior in the electric power plants. Oxygenated treatment (OT) is gradually considered as a more effective chemical water treatment method for ultra-supercritical (USC) unit in comparison with all-volatile treatment (AVT) because it can avoid flow accelerated corrosion (FAC) which occurs in low and high pressure heater[3].

The boiler tube failures caused by corrosion and oxide scale formation in thermal power plants have been investigated by many investigators. Recently, some power plants using OT technique have experienced increased iron concentrations in the drain system of the low-pressure

† Corresponding author: zhangdaquan@shiep.edu.cn

feed-water heater. In addition, a powdered scale deposit has been generated and attached to the inside of the furnace wall tubes, contributing to an increase in the wall tube temperature. Meanwhile, OT-induced exfoliation of oxide scale in steam path is an important problem, which attracts many attentions from the researchers. The exfoliation of oxide scales can cause serious problems such as tube blockages and steam turbine erosion[4]. It is generally accepted that the oxide films of T91 steel consisted of two layers, an outer layer and an inner layer. The porous outer layer forms by the diffusion of iron ions through the Fe–Cr spinel and magnetite layers to the oxide and water vapor interface where an oxidation reaction occurs that accounts for the growth of the outer layer. The denser inner Cr-rich spinel oxide grows by the inward diffusion of oxygen to the oxide and metal interface. The highly defected outer layer allows for rapid oxygen inward diffusion through the magnetite[5].

However, the problems and processes involved in the early stages oxidation of T91 steel are intrinsically different from those involved in the growth of oxide layers in the further oxidation. The corrosion of T91 steel under different water chemistry control conditions and their relationship with the formation of oxide scale is seldom reported. The work presented here is in line with the ongoing programs worldwide particularly in addressing steam-side oxidation of candidate alloys for thermal power plant. The aim of this work is to investigate the relationship between corrosion under different water chemistry control condition and the formation of oxide scale. This will be useful to get the information at the early corrosion stage and evolution of oxide in the further oxidation stage.

2. Experimental Procedure

2.1 Materials

The used steel specimens were from T91 alloy with the following composition (wt%): C 0.08 ~ 0.12; Si 0.20 ~ 0.50; Mn 0.30 ~ 0.60; Cr 9 ~ 12; Mo 0.085 ~ 1.05; V 0.18 ~ 0.25; P ≤ 0.02; S ≤ 0.01; Ni ≤ 0.40 and Fe balance. All reagents were analytical grade and used as received.

2.2 Electrochemical measurements

Electrochemical measurements were performed in a conventional three-electrode cell connected to a computer-controlled electrochemical workstation (Solartron 1287 Electrochemical Interface coupled with a 1260 Impedance/ Gain-Phase Analyzer). Zplot and CorrWare software packages were used for the electrochemical analysis. The electrochemical cell was open to air and the test solution was not stirred or deaerated. The T91 working electrodes (WE) were sealed with epoxy resin so that only the circular cross section (0.5 cm^2) was exposed. Saturated calomel electrode (SCE) was used as reference electrode; the counter electrode was a platinum electrode. EIS measurements were done at the open-circuit potential in the frequency range from 0.02 Hz to100 kHz. A sine wave with 5 mV amplitude was used to perturb the system. Polarization studies were carried out at a scan rate of 0.5 mVs−1. All potentials were presented in mV(SCE).

2.3 SEM and EDS characterization

The steel specimens were immersed in the test solution at 25 ℃ for 1 h. Then the specimens were transferred to a tube furnace for a high temperature oxidization test. The surface microstructure of the different steel specimens was investigated by a scanning electron microscope (SEM) after the corrosion immersion test. An energy dispersive spectroscopy (EDS) was recorded to give the chemical composition of the surface film.

2.4 XRD analysis

X-ray diffraction (XRD) analysis was done using BRUKER-D8 X diffractometer with a step size of 0.1 and with time per step as 7 s. The phases present in the 15CrMo steel specimens before and after the high temperature oxidization test were analyzed by XRD with Cu Kα radiation.

3. Resutls and Discussion

3.1 Electrochemical measurements under different water chemistry condition

In order to control corrosion throughout the steam/water circuits of the electric power plants, it is essential for the technician of the plant to choose and optimize a water chemistry condition. All volatile treatment (AVT) involves the addition of ammonia (or an amine or blend of amines of lower volatility than ammonia) and a reducing agent (usually hydrazine or one of the acceptable substitutes) to the condensate or feedwater of the plant. With oxygenated treatment (OT), oxygen is injected into the feedwater to keep the oxygen level between 30-50 ppb. This forms a thicker protective layer of hematite (Fe_2O_3) on top of the magnetite (Fe_3O_4). OT operation can reduce the risk of flow-accelerated corrosion. In this research, 50 μg/L hydrazine is added and the dissolved oxygen content is controlled below 10 μg/L for AVT condition. The dissolved oxygen content is set at 100 μg/L for OT condition by pumped in pure nitrogen gas. Fig.1 shows the electrochemical impedance plots of T91 electrode after 1 h immersed in different water chemistry

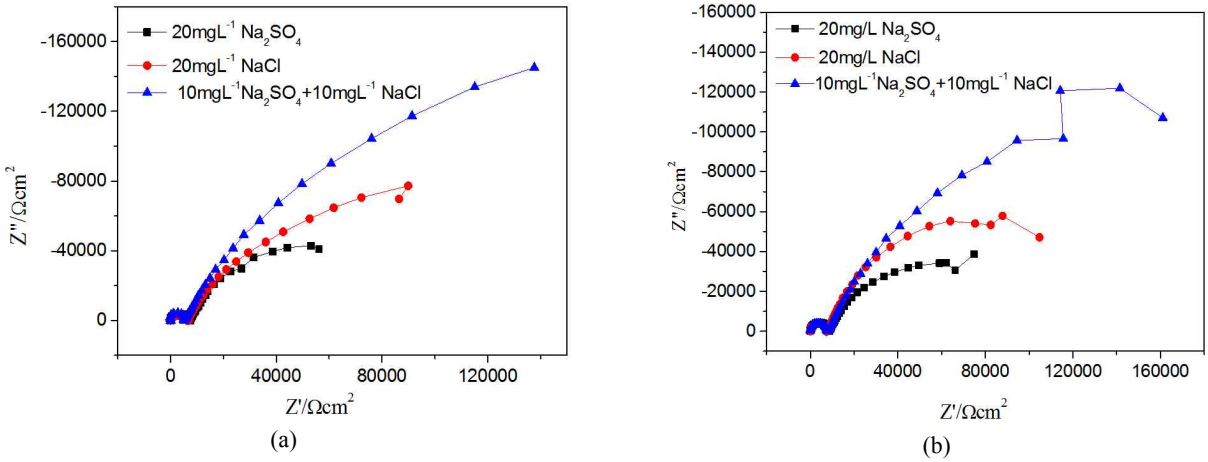

Fig. 1 Nyquist plots of T91 electrode after 1 h immersed in different water chemistry control condition: (a) AVT; (b) OT.

control condition.

As shown in Fig.1a, two capacitive loops in the high frequency and in the low frequency are observed for T91 steel electrode. The high-frequency semicircle is attributed to the parasitic capacitive reactance owing to the reference circuit in the low conductivity solution[6]. Therefore, the impedance plots can be analyzed by the equivalent circuits with the charge-transfer resistance (R_{ct}) paralleling to the double-layer capacitance (C_{dl}). The ZSimpWin software is used for impedance data analysis and the fit parameters are listed in Table1, where Rs stands for the solution resistance.

It is obvious that the T91 electrode under AVT condition has larger R_{ct} values compared to that under OT condition. This indicates that the OT operation need to a strict control of all indexes of water quality. Actually, there is a requirement to stop injecting oxygen into the feedwater if the cation conductivity exceeds 0.3 μS/cm. Under the same water chemistry condition, the SO_4^{2-} ions have the most serious attack effect, for 20 mgL^{-1} Na_2SO_4 leads to the smallest R_{ct} values. It is reported that the initiation of pitting corrosion by SO_4^{2-} ions takes place

Table 1 Electrochemical impedance parameters of T91 steel electrode after 1 h immersed in different water chemistry condition

Water chemistry condition		Rs/Ω·cm^2	C_{dl}/Fcm^{-2} ($\times10^{-5}$)	R_{ct}/kΩ·cm^2
AVT	20 mgL^{-1} Na_2SO_4	7649	7.925	74.98
	20mgL^{-1} NaCl	6934	5.022	116.3
	10 mgL^{-1} Na_2SO_4 +10mgL^{-1} NaCl	5770	3.516	196.7
OT	20 mgL^{-1} Na_2SO_4	9287	5.524	62.54
	20mgL^{-1} NaCl	8166	4.252	101.1
	10 mgL^{-1} Na_2SO_4 +10mgL^{-1} NaCl	8983	2.199	175.6

Table 2 Electrochemical polarization parameters of T91 steel electrode after 1 h immersed under different water chemistry condition

Water chemistry condition		E/V	I_0 /μAcm^{-2}
AVT	20 mgL^{-1} Na_2SO_4	-0.2333	0.22921
	20mgL^{-1} NaCl	-0.2104	0.14618
	10 mgL^{-1} Na_2SO_4 +10mgL^{-1} NaCl	-0.0722	0.10049
OT	20 mgL^{-1} Na_2SO_4	-0.24657	0.27562
	20mgL^{-1} NaCl	-0.24729	0.21201
	10 mgL^{-1} Na_2SO_4 +10mgL^{-1} NaCl	-0.2154	0.06268

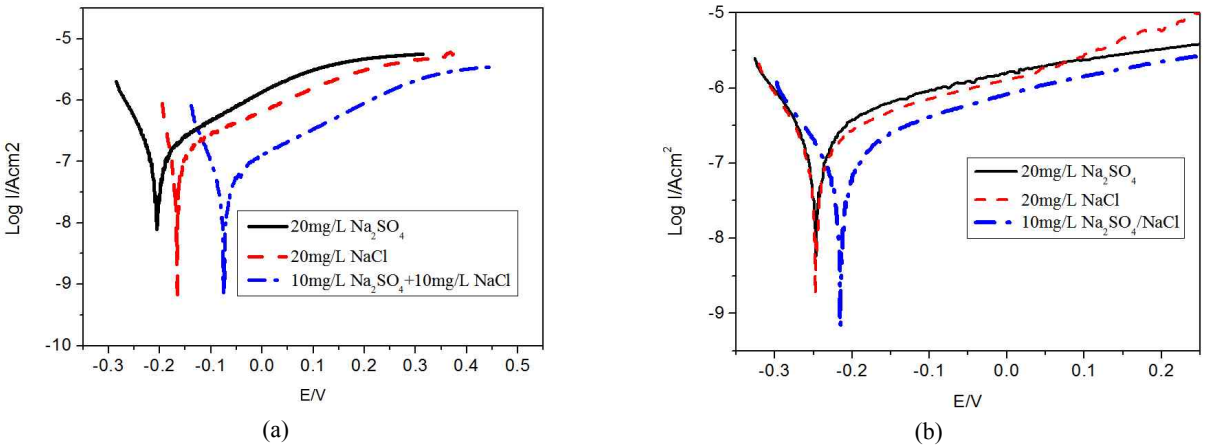

(a) (b)

Fig. 2 Polarization curves of T91 electrode after 1 h immersed under different water chemistry control condition: (a) AVT; (b) OT.

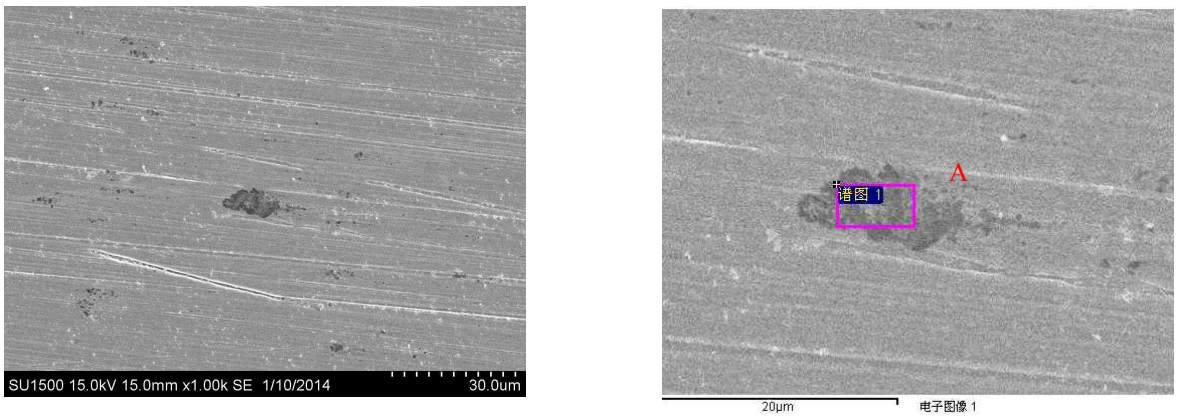

Fig. 3 SEM images of T91 steel after 6 h immersed under AVT condition containing 10 mg/L Na_2SO_4 + 10 mg/L NaCl.

through an adsorption mechanism. The formation of Fe^{2+} is the favored adsorption of SO_4^{2-} ions on oxide films, and creates an electrostatic field across the film/solution interface. When the electrostatic field reaches a certain value, SO_4^{2-} ions penetrate the oxide layer, react with steel at the steel/oxide interface, and promote the local dissolution of T91 steel, resulting in a pit nucleus[7]. From Table 1, the co-existence of Na_2SO_4 and NaCl has an antagonistict effect for corrosion action. This is attributed to the competitive adsorption between SO_4^{2-} ions and Cl^- ions.

Fig.2 shows the electrochemical polarization curves of T91 electrode after 1 h immersed under different water chemistry control condition. The values of E_{corr} and i_{corr} are summarized in Table 2.

It is clear that the presence of SO_4^{2-} ions leads to the most serious corrosion of T91 steel. In the co-existence of Na_2SO_4 and NaCl, T91 steel has the minimum corrosion current densities. This indicates that an antagonistict effect for corrosion action exists between SO_4^{2-} ions and Cl^- ions. The T91 electrode under AVT condition has more positive corrosion potential compared to that under OT condition. It shows that OT operation can not get a passive surface for T91 steel in the presence of corrosive ions, such as SO_4^{2-} and Cl^- [8].

3.2 Surface analysis for T91 steel under different water chemistry condition

3.2.1 SEM and EDS investigation

The microstructure of T91 steel after 6 h immersed under different water chemistry condition containing 10 mg/L

Table 3 The chemical compositions of T91 steel surface obtained by the EDS analysis

Composition/at%	AVT	OT
	"A" spot	"B" spot
C	18.28	43.83
O	64.18	26.18
Si	-	5.28
Cr	2.01	3.00
Fe	15.52	21.71

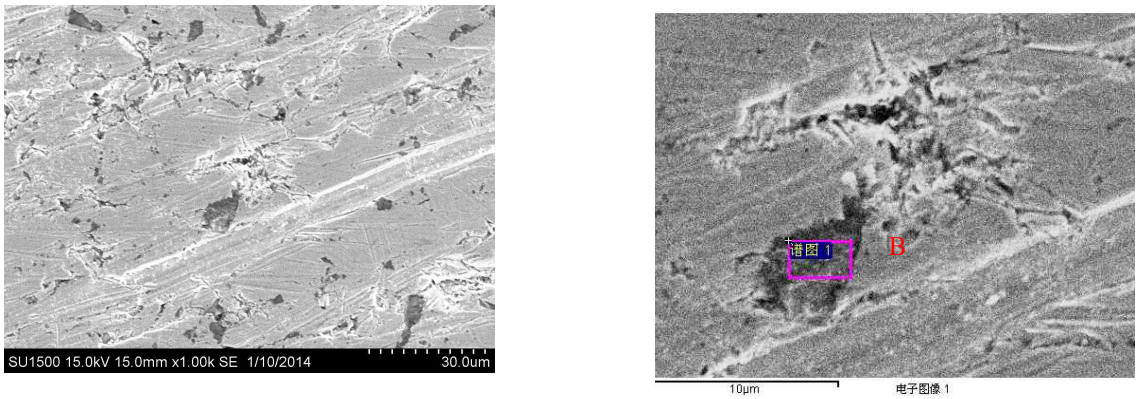

Fig. 4 SEM images of T91 steel after 6 h immersed under OT condition containing 10 mg/L Na_2SO_4 + 10 mg/L NaCl.

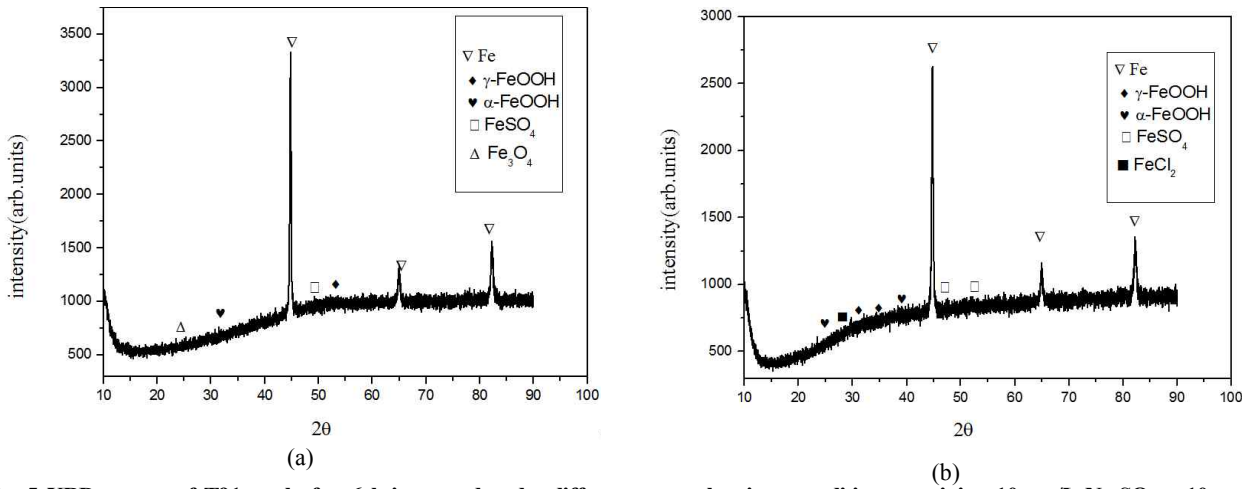

Fig. 5 XRD pattern of T91 steel after 6 h immersed under different water chemistry condition containing 10 mg/L Na_2SO_4 + 10 mg/L NaCl: (a) AVT; (b) OT.

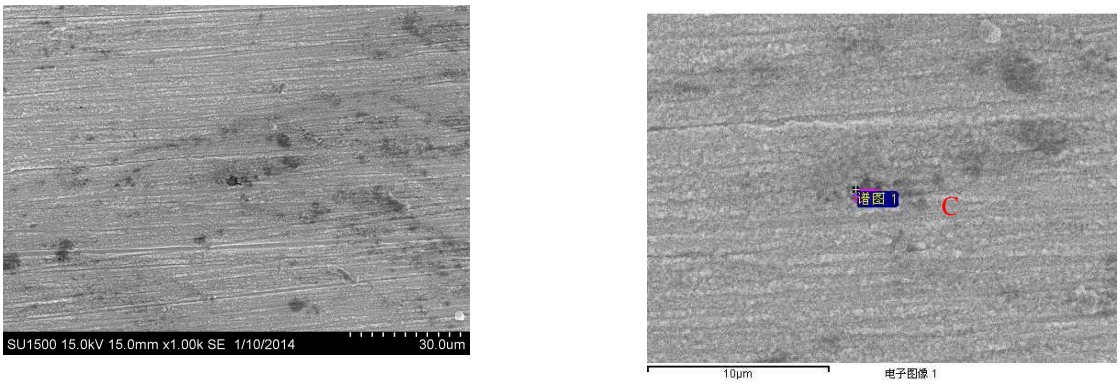

Fig. 6 SEM images of T91 steel after 500 ℃ oxidization for 6 h pretreated by AVT operation.

Na_2SO_4 + 10 mg/L NaCl are shown in Fig.3 and Fig.4. EDS analysis for "A"and "B" spots are shown in Table 3.

The surface of T91 steel has some corrosion pits after 6 h immersion in solution containing 10 mg/L Na_2SO_4 + 10 mg/L NaCl under AVT condition. Meanwhile, there are many corrosion area with cracks on the surface of T91 steel under OT condition. Elemental compositions for "A" spot and "B" spot suggest a higher oxygen concentration, this corresponding to corrosion products[9].

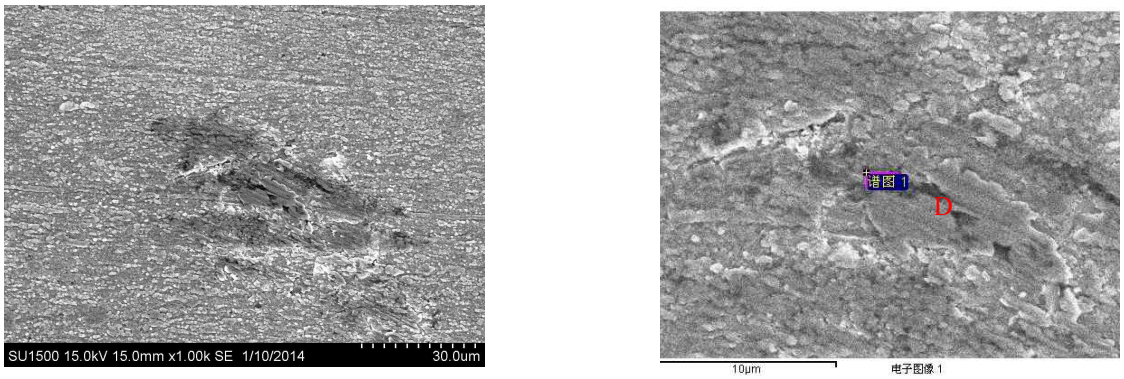

Fig. 7 SEM images of T91 steel oxidized at 500 ℃ for 6 h after pretreated by OT operation.

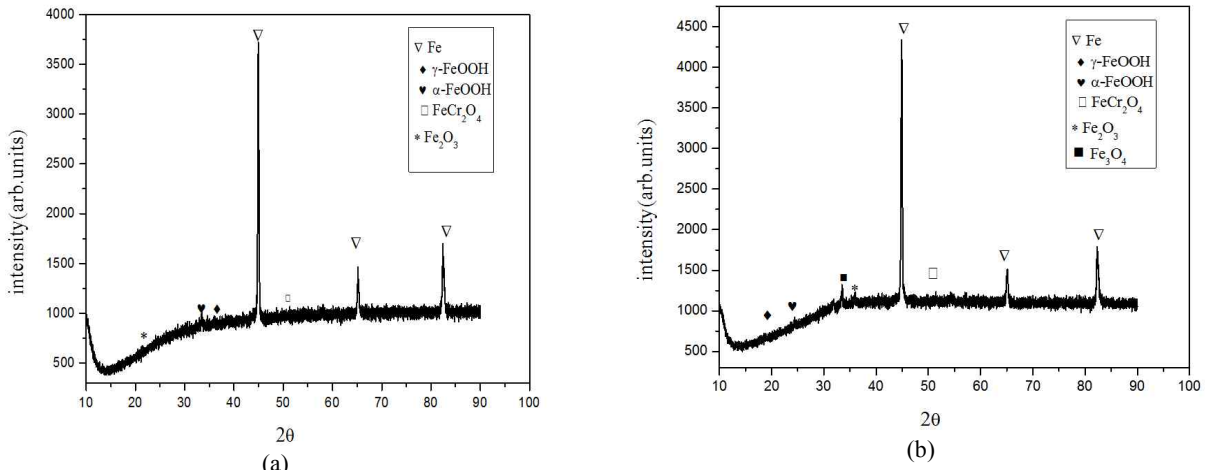

Fig. 8 XRD pattern of T91 steel oxidized at 500 ℃ for 6 h after pretreated by different water chemistry condition: (a) AVT; (b) OT.

3.2.2 XRD analysis

Fig.5 shows the XRD pattern of T91 steel after 6 h immersion in solution containing 10 mg/L Na_2SO_4 + 10 mg/L NaCl under different water chemistry condition. There are no evidence difference in the phase composition of T91 steel after immersed in 10 mg/L Na_2SO_4 + 10 mg/L NaCl solution under AVT or OT condition. The main phase compositions are Fe.

3.3 Surface analysis for T91 steel after high-temperature oxidization test

3.3.1 SEM and EDS investigation

The T91 steel was immersed in solution containing 10 mg/L Na_2SO_4 + 10 mg/L NaCl for 6 h under different water chemistry condition. Then the specimens were transferred to be oxidized at 500 ℃ under air condition in tube-furnace for 6 h. SEM images for the high temperature oxidation specimens are illustrated in Fig.6 and Fig.7. EDS analysis for "C"and "D" spots is shown in Table 4.

It is found that the oxide film on T91 surface after 500 ℃ oxidization has a multi-layer structure. The oxide film is easy to peel off from the surface of T91 steel for OT operation compare to that for AVT operation. There is an oxide film with many cracks on T91 surface under OT operation. The pre-corrosion under different water chemistry condition gives a change for the oxide scale structure formed by the high-temperature oxidation.

Table 4 The chemical compositions of T91 steel surface obtained by the EDS analysis

Composition / wt%	AVT	OT
	"C" spot	"D" spot
C	8.2	10.06
O	53.95	34.52
Cr	4.02	8.94
Fe	33.35	46.48

Elemental compositions of "C" spot and "D" spot suggest that they corresponds to corrosion products. The higher Cr content for OT operation compared to that for AVT operation is observed. These indicate that the more oxide film formed for OT operation after high temperature oxidation test.

3.3.2 XRD analysis

Fig.8 shows the XRD pattern of different water chemistry pretreated T91 steel after 500 ℃ oxidization for 6 h.

There is no evidence difference in the phase composition of T91 steel after 500 ℃ oxidization for 6 h under AVT or OT condition. The main phase compositions are Fe and Fe_2O_3. The presence of Fe_3O_4 for OT operation represents the cracked multilayer oxide film. It has been reported that the oxide scale was constituted by a layered (or duplex) structure, composed of Fe and Cr oxides[10]. The outer layer is predominantly iron oxides, whereas the innermost layer contains significant amount of chromium. The OT operation with the contamination of SO_4^{2-} and Cl^- ions brings a high cracked oxide scale.

4. Conclusions or Summary

The SO_4^{2-} and Cl^- ions initiate the corrosion of T91 steel under both AVT and OT operation. Under the same water chemistry condition, the SO_4^{2-} ions have the most serious attack effect. The co-existence of Na_2SO_4 and NaCl has an antagonistict effect for corrosion action. In the presence of erosion ions, such as SO_4^{2-} and Cl^-, OT operation aggravates the corrosion of T91 steel compared to AVT operation. The OT operation with the contamination of SO_4^{2-} and Cl^- ions brings a high cracked oxide scale after high oxidation test.

Acknowledgments

We are grateful to supports from Shanghai S&T Committee project (11JC1404400, 14DZ0500700, 14DZ2261000), and from Shanghai Key Laboratory of Materials Protection and Advanced Materials in Electric Power.

References

1. R. Viswanathan, J. Sarver, and J. M. Tanzosh, *J. Mater. Eng. Perform.*, **15**, 255 (2006).
2. D. A. Guzonas and W. G. Cook, *Corros. Sci.*, **65**, 48 (2012).
3. B. C. Syret, *Corros. Sci.*, **35**, 1189 (1993).
4. YY. Kaiju, Q. Shaoyu, T. Rui, Z. Qiang, and Z. Lefu., *J. Supercrit. Fluid.*, **50**, 235 (2009).
5. J.-L. Huang, K.-Y. Zhou, J.-Q. Xu, and C.-X. Bian, *J. Loss Prevent. Proc.*, **26**, 22 (2013).
6. Y. Feng, G. Zhou, and S. Cai, *Electrochim. Acta*, **36**, 1093 (1991).
7. S. Xiong, Z. Zhu, H. Zhang, and L. Jing, *Corrosion*, **68**, 1 (2012).
8. D. Laverde, T. Gómez-Acebo, and F. Castro, *Corros. Sci.*, **46**, 613 (2004).
9. J. L. Huang, K. Y. Zhou, and J. Q. Xu, *Mater. Corros.*, **65**, 786 (2015).
10. Y. Chen, K. Sridharan, and T. Allen, *Corros. Sci.,* **48**, 2843 (2006).